Constraining Solar Wind Heating Processes by Kinetic Properties of Heavy Ions

Patrick J. Tracy, Justin C. Kasper, Jim M. Raines, Paul Shearer, Jason A. Gilbert, and Thomas H. Zurbuchen

Phys. Rev. Lett. **116**, 255101 — Published 21 June 2016

DOI: 10.1103/PhysRevLett.116.255101

Constraining solar wind heating processes by kinetic properties of heavy ions

4/21/2016

Patrick J. Tracy[*1], Justin C. Kasper[1], Jim M. Raines[1], Paul Shearer[1], Jason A. Gilbert[1], and Thomas H. Zurbuchen[1]

1-Department of Climate and Space Sciences and Engineering, University of Michigan, Ann Arbor, MI, USA
*Contact: ptracy@umich.edu

Abstract

We analyze the heavy ion components (A > 4 amu) in collisionally young solar wind plasma and show that there is a clear, stable dependence of temperature on mass, probably reflecting the conditions in the solar corona. We consider both linear and power law forms for the dependence and find that a simple linear fit of the form $T_i/T_p = (1.35 \pm .02) m_i/m_p$ describes the observations twice as well as the equivalent best fit power law of the form $T_i/T_p = (m_i/m_p)^{1.07 \pm .01}$. Most importantly we find that current model predictions based on turbulent transport and kinetic dissipation are in agreement with observed non-thermal heating in intermediate collisional age plasma for $m/q < 3.5$, but are not in quantitative or qualitative agreement with the lowest collisional age results. These dependencies provide new constraints on the physics of ion heating in multi-species plasmas, along with predictions to be tested by the upcoming Solar Probe Plus and Solar Orbiter missions to the near-Sun environment.

Introduction

The solar corona has a temperature that far exceeds that of the photosphere and results in the acceleration of the coronal plasma into the supersonic and super-Alfvénic solar wind [1,2]. The physical processes responsible for this heating and acceleration have been the subject of experimental and theoretical study for more than half a century. Many proposed mechanisms require interactions between fluctuations and particles on short kinetic scales comparable to the gyroradii of the constituent species of the plasma. This is a particularly challenging plasma regime to observe and to model because it occurs at scales where fluid approximations break down and kinetic descriptions of the plasma are needed.

Several of the most promising theories that seek to explain ion heating in the corona and solar wind use the dissipation of fluctuations via wave-particle interactions on kinetic scales such as ion-cyclotron resonance [3,4], stochastic heating by long wavelength kinetic Alfvén waves [5], or the interaction of particles with localized structures such as current sheets or topological null-points emerging through turbulence [6-8]. Theories that preferentially act on different species are motivated by the observed non-thermal nature of the near-corona (< several solar radii) from spectroscopy [9], and the fact that temperatures of observed ion species and electrons are different when directly observed in interplanetary space by instruments on spacecraft [10].

Multiple models have been reported to be qualitatively and even quantitatively consistent with in situ measurements of protons (H^+) and alpha particles (He^{2+}), which constitute over 99.9% of the particle density of the solar wind [5,11]. Furthermore, alpha particles account for 20% or more of the internal

energy in these measurements [12], causing them to have an important effect on the dispersion relations relevant for wave-particle interactions and complicating their use in evaluation of heating theories [13]. Heavy ions (A > 4 amu) can further constrain the physical mechanisms. With number densities several orders of magnitude lower than alpha particles, they are an excellent approximation to test particles, responding to wave-particle interactions throughout the inner heliosphere without causing significant changes to the expansion and acceleration of the solar wind itself [14].

Extensive studies have demonstrated that the occurrence of non-thermal kinetic effects in the solar wind is strongly limited by the cumulative effects of Coulomb collisions occurring as the wind travels from the corona to interplanetary space [11,15-18]. The net effect of these heating and thermalization processes has been extensively studied with the alpha particle population in the solar wind [15], and Coulomb collisional relaxation has recently been shown to also be important for the heavy ion populations [18]. By examining the temperature ratios of heavy ions relative to protons, organized by the collisional thermalization of the plasma, we can reveal several important features of the heavy ion heating present in the solar wind, and provide crucial constraints on the proposed heating theories in the solar wind. This is critical because the Coulomb collision frequency is a function of the charge and mass of the ions involved, and different levels of collisional relaxation could be misinterpreted as evidence of a particular charge or mass ordering of ion temperatures. Previous studies of heavy ion kinetics have not explicitly accounted for the effects of collisional thermalization in reports of trends in ion temperatures [14].

Our methodology is to search for evidence that an asymptotic ordering of ion temperatures by mass and charge characteristics is achieved when we examine solar wind with decreasing levels of Coulomb thermalization. The initial relative temperature state between solar wind ion species is reflected in these plasma parcels with the lowest collisional thermalization [11]. Assuming negligible heating during their subsequent propagation to 1 AU and equal relative cooling due to similar adiabatic expansion effects, these parcels preserve the initial temperature ratios of the solar wind, created in some critical radial distance from the Sun. There has been observational evidence that all solar wind converges to a single non-thermal state after collisional effects are removed [16], supporting the assertion that most preferential ion heating occurs near the Sun, followed by expansion and collisional relaxation.

Observations and Analysis

We use the techniques described in Tracy et al. [18] to examine the kinetic behavior of heavy ions in the solar wind and relate it to the collisional age [15] of each two-hour measurement interval of solar wind plasma made by ACE/SWICS at 1 AU. The second moment of the reduced velocity distribution function measured by the ACE/SWICS main and H/He channels [18,19] is used to estimate the thermal velocity of the heavy ions and protons, respectively. This work extends that analysis to the 11 most abundant heavy ions in the solar wind, which we select from over 70 different measured ions, chosen for the high signal to noise of the measured distribution functions. We require that at least 100 particles are measured for a given ion charge state within a two hour interval before we calculate our moments, preventing the inclusion of scarcer solar wind ions in this study. In total, about 50,000 two hour intervals collected by ACE between 1998-2011 form the basis of this study. A critical aspect of this analysis is the use of a statistical inversion procedure to account for the fact that these particle populations do not have sufficient count rates to warrant Gaussian errors and because most of the ion

peaks partially overlap with other species. Previously published results [20,21] are based on simplifying assumptions that are not generally justifiable for this analysis [19]. One must also note that the calculation of the second moment used in this work is a moment of the entire distribution, which will include suprathermal tails and other features. Filtering these tails out of the moments can result in thermal velocities up to 10-15% smaller than the full moment method, in some cases.

In Figure 1 we show the median value of $v_{th,i}/v_{th,p}$, the ratio of the most probable thermal speed of each species to the proton thermal speed, as a function of collisional age A_C. The specifics of A_C are defined in [15] and involve calculating the timescale for Coulomb thermalization between each species and protons compared to the time it takes for the solar wind to reach 1 AU, assuming constant speed and collision frequencies. It is an approximation, but has been shown to order the data well [15,18]. Note that A_C must be calculated separately for each of the heavy ion species analyzed. Each heavy ion curve is only shown over the extent in A_C where it had at least 100 valid measurements at each A_C bin [18]. For most points shown in this figure far more than 100 points are included in the calculations.

The typical median absolute deviation (MAD) is shown for O^{6+} ($\sigma_{O^{6+}}$). This value can be fairly large relative to the separation between the ion curves, and is representative of the MAD seen for other ion species. A large variety of physical processes apart from collisional relaxation, governed by factors like differential streaming or plasma beta [5,11], drive the observed variability in the solar wind. With the current data set we cannot accurately filter for these other processes whose contributions result in a MAD that is an overestimate of the actual measurement uncertainty. Note that the uncertainty in the median value $\left(\frac{\sigma_{O^{6+}}}{\sqrt{N}}\right)$ is small relative to the separation between ion curves, with the uncertainty bars being less than the width of the points shown on each curve. The physically relevant measurement uncertainty is somewhere between these extremes. The clear overall trend in the observations is the highly unequal and elevated heavy ion thermal velocities at low A_C, gradually decaying towards thermal equilibrium with protons as A_C increases.

It is interesting that some heavy ions do not show a simple monotonic exponential decay toward equal temperature with protons as collisional age increases as would be expected from simple Coulomb relaxation. In particular, for heavy ions with *m/q* around 3 amu/e, e.g. O^{6+}, we see a distinct enhancement to higher thermal velocity ratios around A_C = 0.1 before the eventual decay toward thermal equilibrium. This figure verifies that heavy ion temperatures in the solar wind are strongly affected by Coulomb collisional thermalization, even if that alone cannot explain the trend of $v_{th,i}/v_{th,p}$ with A_C for all heavy ions.

Figure 2 is presented in the same format as Figure 1, except we show the temperature ratio, T_i/T_p, of heavy ions to protons. At the lowest collisional ages heavy ions are far from thermal equilibrium, and Coulomb collisional thermalization has a large effect on decreasing these temperature ratios toward unity. Note that there are very few measurements of unity values for T_i/T_p in the SWICS data set. This appears to be in contrast to other data sets at 1 AU [15], which observe a significant number of events with alphas and protons at equal temperatures. It is possible that SWICS cannot resolve equal temperatures due to its energy resolution [18], or differences in how temperatures are calculated, since prior studies have shown that differences in algorithms can lead to errors in temperature [22]. In any case, this is an issue at high collisional age (high A_C) and does not affect the primary conclusions of this

work, which is behavior at small A_C. However, the mean values of the ratios at large A_C are useful indicators of the approximate error of these temperature ratio measurements if they indeed should be approaching unity.

As Coulomb thermalization has such a large effect on the observed heavy ion kinetics, we must look at Figures 1 and 2 at different values of A_C to understand the evolution of trends in heavy ion temperatures. Three intervals of A_C are highlighted in blue in the previous figures and are examined in Figure 3. In Figure 3a we display the median value of the temperature ratio between heavy ions and protons at several values of A_C, ordered by the mass of the heavy ion. The specific A_C ranges are indicated in the legend, and the black line is a reference curve for strictly mass proportional temperatures. For both the lowest and the intermediate collisional age ranges a strong organization of the heavy ion temperatures by their mass is clear.

Examining the same collisional age ranges, we look at the thermal velocity ratio between the heavy ions and protons in Figure 3b. The thermal velocity ratio effectively divides out the mass dependence shown in Figure 3a, revealing additional orderings in the observed plasma heating. The thermal velocity ratio vs *m/*q value of the heavy ions appears to show an inverse relation at the lowest A_C, but a positive correlation for a subset of the intermediate A_C group. This is particularly interesting as most wave heating theories predict that this ratio should increase with increasing *m/*q values. We have plotted one such prediction from Chandran et al. [5] for how the thermal velocity ratio scales with *m/q* to show the discrepancy. The lowest A_C range does not well match the prediction, but the intermediate A_C range agrees well for $m/q < 3.5$. The fact that the data points of the intermediate A_C group lie below the predicted curve for m/q<3.5 is likely a result of the marginal relaxation implied by their collisional age. However, if one were to just focus on the He^{2+} (m/q=2) measurements it would appear that both the low A_C and intermediate A_C ranges agree with the predicted curve. It must be noted that this prediction is only valid for low beta plasmas, and we have not filtered our data to meet this requirement, as we don't know what the value of plasma beta was in the outer corona where these temperature ratios presumably were set.

The importance of looking at low collisional age plasmas is made apparent in Figure 3, where we see a significant alteration of the trends present from 3a and 3b for the highest collisional age shown (triangles). The mass proportionality in 3a is much diminished and the thermal velocity organization in 3b has completely disappeared for the high A_C range. In Figure 4 we present the recovered parameters for a linear fit to the T_i/T_p vs m curve at each collisional age in our data set (three of which are displayed in Figure 3a). In Figure 4, we see that in the lowest collisional age wind, the proportionality factor between temperature ratio and mass ratio is about $1.35\pm.02$. We also performed a power law fit (not shown), which yields an exponent of $1.07\pm.01$ at the lowest collisional age values.

Both the linear and power law fit suggest that the temperature dependence on mass in collisionless solar wind has a proportionality factor greater than unity. By visual inspection we cannot readily distinguish whether linear or power-law models better describe our data, but we can compare the reduced χ^2 values for the two models. The reduced χ^2 values for the lower collisional age range vary from 0.4-0.6 for the linear fit and from 0.9 to 1.2 for the power law fit, indicating that the linear fit does twice as well reproducing the temperatures than the power law. **As we have conservatively**

overestimated the error with the MAD, we expect the reduced χ^2 values for a model consistent with observations to be below unity. The coefficient of determination, R^2, of the fits also shows that the linear fit is superior at low collisional ages, but that both fits show a decreasing R^2 value with increasing collisional age. This shows that either of the fits to the ion temperatures works best at low collisional ages.

Conclusions

The thermal properties of heavy ions in the solar wind, comprehensively presented in this paper for the first time as functions of Coulomb collisional age, mass, and mass per charge, provide important constraints on heating theories of coronal and solar wind plasma. The linear dependence of heavy ion temperatures on mass shows a distinct asymptote to $1.35 \pm .02$ in the absence of significant Coulomb collisions. This asymptotic value has not been reported before and we propose it is indicative of the typical coronal mass dependence of ion temperatures, and is not necessarily produced by local heating in the solar wind in interplanetary space. The slope of the linear dependence is gradually decreased in more collisional solar wind. We suggest that prior studies of the ordering of ion temperatures in the solar wind that did not account for Coulomb relaxation were reporting a mix of the effects of non-thermal heating and Coulomb collisions. Not all heavy ions undergo a simple monotonic and exponential decay toward equal temperatures with increasing A_C (e.g. O^{6+}, N^{5+}, C^{4+}). This deviation may be a valuable signature of additional heating occurring between the corona and interplanetary space, or reflect the presence of two solar wind populations with different asymptotic values at low A_C.

Of equal interest is that we show for the first time the ordering of heavy ion thermal velocity ratios by *m/q*, accounting for collisional effects. **We find that heavy ion thermal velocities do not increase with *m/q* in low A_C wind, in disagreement with several heating theories for the solar wind.** The ion cyclotron resonance [11] and stochastic heating by low frequency turbulence [5] should both have a larger impact on ions with larger *m/q* values. However, for intermediate A_C, which coincides with the deviation from simple exponential decay in Figures 1-2, the heavy ion thermal velocities agree fairly well with their predicted *m/q* dependence for *m/q*<3.5 [5]. **It is intriguing that the highest m/q ions show no trend with m/q for any collisional age.** It is crucial to note that if one were to just look at the He^{2+} (*m/q*=2) population relative to the protons in Figure 3b, it would appear that the heating of He^{2+} is in rough agreement with the *m/q* dependence predicted by Chandran et al. [5] for both the low and intermediate A_C ranges. This emphasizes the need to examine heavy ions, which can act as test particles in the solar wind and may reveal different aspects of the heating mechanisms present.

Solar Probe Plus, a spacecraft that will traverse from 1 AU to 9.86 solar radii from the Sun will be able to directly observe the evolution of the solar wind as it propagates to 1 AU. Solar Probe will measure the non-thermal properties of a limited set of ions during the entire orbit [23], perhaps comparable to the data reported by Gershman et al. [24]. The upcoming Solar Orbiter mission will carry an instrument allowing independent mass and charge measurements of heavy ions as presented here, but it will not venture nearly as close to the Sun, ranging 0.29-1.4 AU. Combining heavy ion plasma measurements at 1 AU with these upcoming missions should allow significant progress in understanding heavy ion thermalization and plasma heating in the solar wind.

The results discussed here also have important consequences for the understanding of other astrophysical plasmas [25,26]. Many remote diagnostics of the thermal state of energetic plasma such as supernovae remnants and accretion disks rely on x-ray spectroscopy of trace ions such as oxygen and iron. As we have demonstrated, in the absence of strong Coulomb collisions on the dynamical scale of the shock or accretion flow, these trace ions may have significantly different plasma properties than the protons, which carry the momentum and most of the energy of the plasma. It is instructive to note for our Sun that –despite having a metallicity of approximately 2% [27] – heavy ions carry approximately 4% of the internal energy and 3% of the momentum of the solar wind to be added to 20% of energy and momentum for alphas. In the near-solar environment, if observations such as Kohl et al. [28] are correct, these numbers might be as high as 14% of the internal energy and 4% of momentum for the heavy ions.

Acknowledgement: We acknowledge the many individuals who have built SWICS and have participated in the generation of the data that are used here. This work was supported, in part, by NASA grant NNX13AH66G and NNX13AO68H.

References

[1] Kuperus, M., Ionson, J.A., Spicer, D.S., Ann. Rev. Astron. Astrophys., **19**, 7-40 (1981)
[2] Parker, E.N., ApJ, **128**, 664 (1958)
[3] Isenberg, P.A., & Vasquez, B.J., ApJ, **696**, 591 (2009)
[4] Cranmer, S.R., van Ballegooijen, A.A., ApJ, **754**, 92 (2012)
[5] Chandran, B.D.G., Verscharen, D., Quataert, E., et al., ApJ, **776**, 45 (2013)
[6] Osman, K.T., Matthaeus, W.H., Greco, A., Servidio, S., ApJ, **727**, L11 (2011)
[7] Osman, K.T., Matthaeus, W.H., Wan, M., Rappazzo, A.F., Phys. Rev. Lett., **108**, 261102 (2012)
[8] Greco, A., Matthaeus, W.H., Servidio, S., Chuychai, P., Dmitruk, P., ApJ, **691**, L111 (2009)
[9] Landi, E., & Cranmer, S.R., ApJ, **691**, 794 (2009)
[10] Newbury, J.A., Russell, C.T., Phillips, J.L., Gary, S.P., J. Geophys, Res., **103**, 9553 (1998)
[11] Kasper, J.C., Bennett, M.A., Stevens, M.L., Zaslavsky, A., Phys. Rev. Lett., **110**, 091102 (2013)
[12] McKenzie, J.F., Banaszkiewicz, M., and Axford, W.I., Astron. and Astrophys., **303**, L45-L48 (1995)
[13] Isenberg, P.A., J. Geophys. Res., **89**, 2133 (1984)
[14] von Steiger, R., & Zurbuchen, T.H., Geophys. Res. Lett., **33**, L09103 (2006)
[15] Kasper, J.C., Lazarus, A.J., Gary, S.P., Phys. Rev. Lett., **101**, 261103 (2008)
[16] Maruca, B.A., Bale, S.D., Sorriso-Valvo, L., Kasper, J.C., Stevens, M.L., Phys Rev. Lett., **111**, 241101 (2013)
[17] Hefti, S., Gründwaldt, H., Ipavich, F. M., et al., JGRA, **103**, 29697 (1998)
[18] Tracy, P.J., Kasper, J.C., Zurbuchen, T.H., et al., ApJ, **812**, 170 (2015)
[19] Shearer, P., von Steiger, R., Raines, J.M., et al., ApJ, **789:60** (10pp) (2014)
[20] von Steiger, R., Schwadron, N., Fisk, L.A., et al., J. Geophys. Res, **105**, 27217 (2000)
[21] Wimmer-Schweingruber, R.F., von Steiger, R., Geiss, et al., Space. Sci. Rev., **85**, 387-396 (1998)
[22] Kasper, J.C., Lazarus, A.J., Steinberg, J.T., Ogilvie, K.W., Szabo, A., JGR, **111**, A03105
[23] Kasper, J.C., Abiad, R., Austin, G., et al., SSRv, doi:10.1007/s11214-015-0206-3
[24] Gershman, D.J., Zurbuchen, T.H., Fisk, L.A., et al., JGRA, **117**, A00M02 (2012)
[25] Safi-Harb, S., et al., ApJ, **545**, 922-938 (2000)
[26] Romero, G.E., Vieyro, F.L., and Vila G.S., Astron. and Astrophys., **519**, A109 (2010)
[27] von Steiger, R., & Zurbuchen, T.H., ApJ, **816**:**13** (8pp) (2016)
[28] Kohl, J.L., et al., ApJ, **501**, L127-L131, doi:10.1086/311434 (1998)

Figure Captions

Figure 1: The median value of ion thermal speed ratio $v_{th,i}/v_{th,p}$ as a function of collisional age, A_C , for several heavy ions measured in the solar wind. The median absolute deviation is shown as errorbars for O6+ and is representative of the variability of the data for the other ions. Subintervals over specified collisional age ranges used in subsequent analysis are highlighted in blue.

Figure 2: The median value of T_i/T_p as a function of collisional age, A_C, for several heavy ions measured in the solar wind. The median absolute deviation is shown as errorbars for O^{6+} and is representative of the variability of that data for the other ions. Subintervals are highlighted as in Figure 1.

Figure 3: In a) the ratio T_i/T_p is plotted vs the mass of heavy ions, for plasma with collisional age ranges indicated in the plot legend. In b), the ratio $v_{th,i}/v_{th,p}$ is plotted against the mass per charge ratio of ion i, for the same collisional age ranges as in a). The ions included are He^{2+}, O^{6-7+}, C^{4-6+}, N^{5+}, Ne^{8+}, Si^{8+}, and Fe^{9-10+}. The MAD values for the data points shown are the same as those in Figures 1 and 2 for $v_{th,i}/v_{th,p}$ and T_i/T_p, respectively.

Figure 4: The slope of the linear fit to the T_i/T_p vs *m* curves at all collisional ages is shown, along with the 95% confidence interval of the recovered slope as a vertical error bar, and the histogram bin width over A_C as the horizontal error bar. The uncertainty weighted average and uncertainty in that average for all collisional age bins less than 0.1 is also inset on the figure.

Figure 1

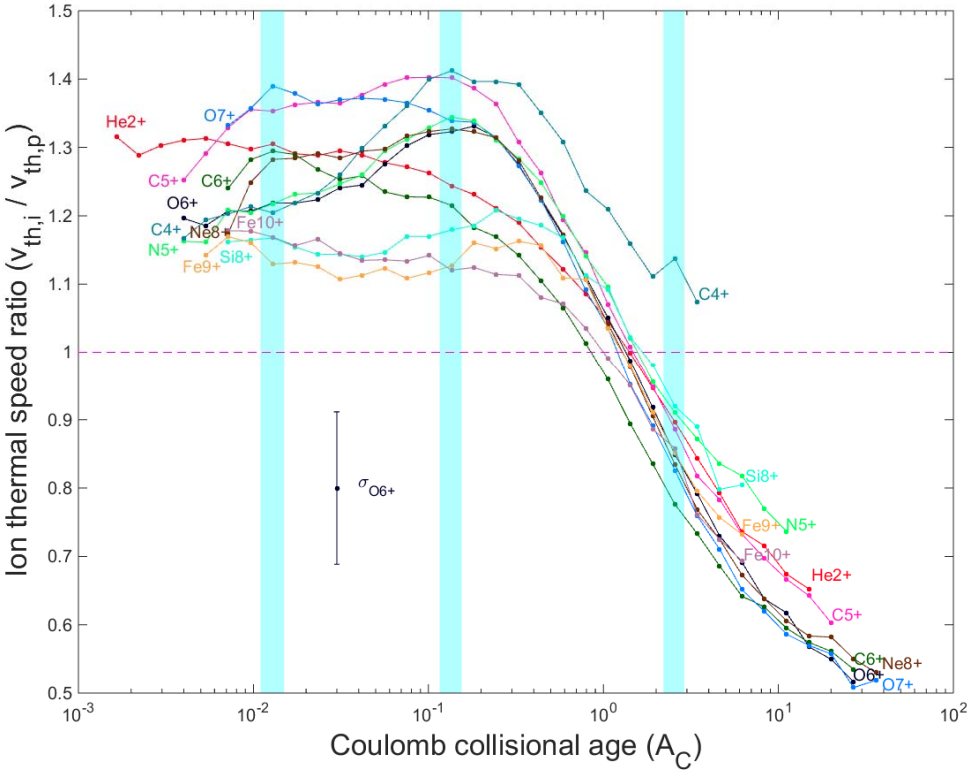
Ion thermal speed ratio ($v_{th,i}$ / $v_{th,p}$)
Coulomb collisional age (A_C)
1.5
1.4
1.3
1.2
1.1
1
0.9
0.8
0.7
0.6
0.5
10^{-3}
10^{-2}
10^{-1}
10^{0}
10^{1}
10^{2}
He2+
O7+
C5+
C6+
O6+
C4+
Ne8+
Fe10+
N5+
Si8+
Fe9+
σ_{O6+}
C4+
Si8+
Fe9+
N5+
Fe10+
He2+
C5+
C6+
Ne8+
O6+
O7+

Figure 2

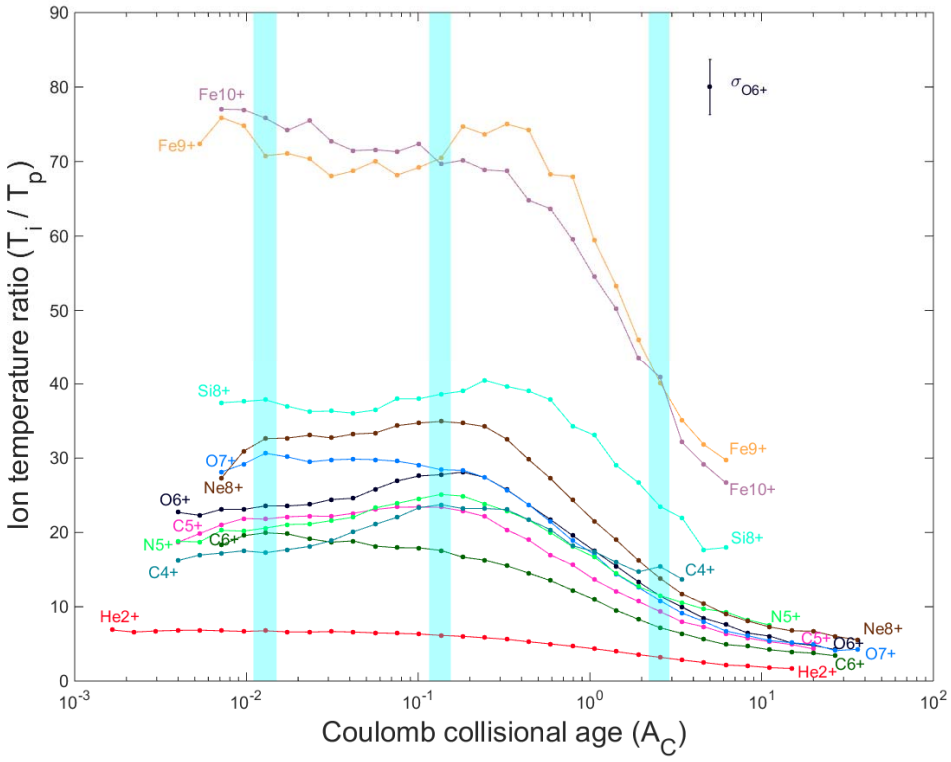

Figure 3

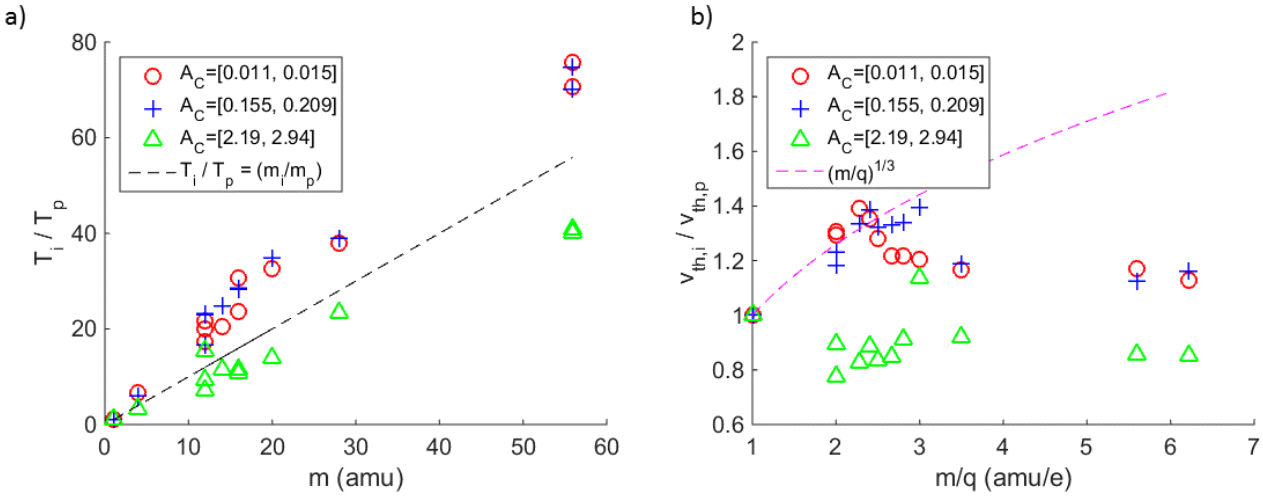

Figure 4

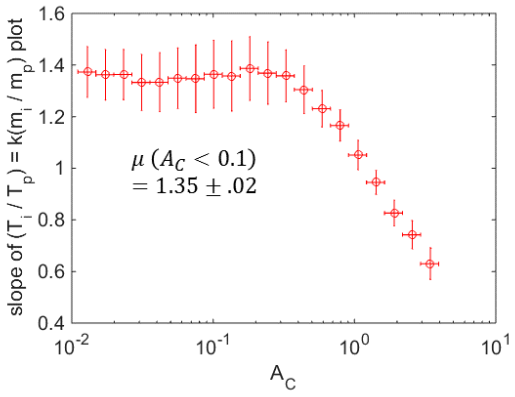
slope of (T_i / T_p) = k(m_i / m_p) plot
1.6
1.4
1.2
1
0.8
0.6
0.4
10^-2
10^-1
10^0
10^1
A_C
μ (A_C < 0.1)
= 1.35 ± .02